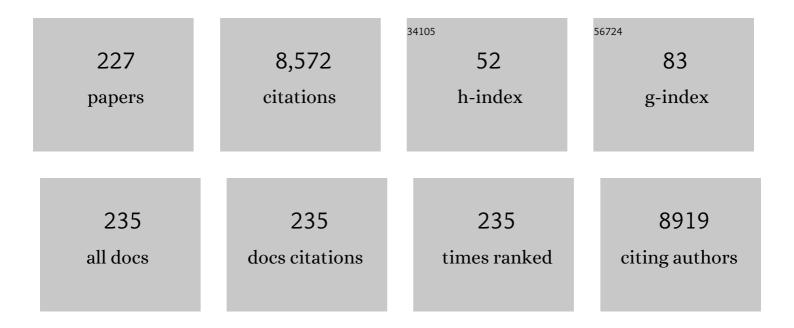
List of Publications by Year in descending order

Source: https://exaly.com/author-pdf/203230/publications.pdf Version: 2024-02-01



#	Article	IF	CITATIONS
1	An <sup>89</sup> Zr-Labeled PSMA Tracer for PET/CT Imaging of Prostate Cancer Patients. Journal of Nuclear Medicine, 2022, 63, 573-583.	5.0	17
2	Translational Development of a Zr-89-Labeled Inhibitor of Prostate-specific Membrane Antigen for PET Imaging in Prostate Cancer. Molecular Imaging and Biology, 2022, 24, 115-125.	2.6	10
3	Imaging of cerebral tryptophan metabolism using 7-[18F]FTrp-PET in a unilateral Parkinsonian rat model. NeuroImage, 2022, 247, 118842.	4.2	2
4	mGluR5 binding changes during a mismatch negativity task in a multimodal protocol with [11C]ABP688 PET/MR-EEG. Translational Psychiatry, 2022, 12, 6.	4.8	7
5	<scp>mGluR<sub>5</sub></scp> and <scp>GABA<sub>A</sub></scp> receptorâ€specific parametric <scp>PET</scp> atlas construction— <scp>PET</scp> / <scp>MR</scp> data processing pipeline, validation, and application. Human Brain Mapping, 2022, 43, 2148-2163.	3.6	5
6	Positron Emission Intensity in the Decay of 86gY for Use in Dosimetry Studies. Molecules, 2022, 27, 768.	3.8	4
7	Age and Anterior Basal Forebrain Volume Predict the Cholinergic Deficit in Patients with Mild Cognitive Impairment due to Alzheimer's Disease. Journal of Alzheimer's Disease, 2022, , 1-16.	2.6	3
8	Assessment of the In Vivo Relationship Between Cerebral Hypometabolism, Tau Deposition, TSPO Expression, and Synaptic Density in a Tauopathy Mouse Model: a Multi-tracer PET Study. Molecular Neurobiology, 2022, 59, 3402-3413.	4.0	10
9	Excitation functions of proton-induced nuclear reactions on \$\$^{86}\$\$Sr, with particular emphasis on the formation of isomeric states in \$\$^{86}\$\$Y and \$\$^{85}\$\$Y. European Physical Journal A, 2022, 58, 1.	2.5	3
10	Cyclotrons Operated for Nuclear Medicine and Radiopharmacy in the German Speaking D-A-CH Countries: An Update on Current Status and Trends. Frontiers in Nuclear Medicine, 2022, 2, .	1.2	3
11	Convenient PET-tracer production via SuFEx 18F-fluorination of nanomolar precursor amounts. European Journal of Medicinal Chemistry, 2022, 237, 114383.	5.5	12
12	18F-Labelled probes for non-invasive assessment of the IDH genotype in glioma patients. Nuklearmedizin - NuclearMedicine, 2022, 61, .	0.7	0
13	The role of chemistry in accelerator-based production and separation of radionuclides as basis for radiolabelled compounds for medical applications. Radiochimica Acta, 2022, 110, 707-724.	1.2	1
14	Two Decades of Brain Tumour Imaging with O-(2-[18F]fluoroethyl)-L-tyrosine PET: The Forschungszentrum Jülich Experience. Cancers, 2022, 14, 3336.	3.7	8
15	One-Stop Shop: <sup>18</sup> F-Flortaucipir PET Differentiates Amyloid-Positive and -Negative Forms of Neurodegenerative Diseases. Journal of Nuclear Medicine, 2021, 62, 240-246.	5.0	18
16	Current trends in the use of O-(2-[18F]fluoroethyl)-L-tyrosine ([18F]FET) in neurooncology. Nuclear Medicine and Biology, 2021, 92, 78-84.	0.6	30
17	Expanding PET-applications in life sciences with positron-emitters beyond fluorine-18. Nuclear Medicine and Biology, 2021, 92, 241-269.	0.6	19
18	Radiosynthesis and evaluation of 18F-labeled dopamine D4-receptor ligands. Nuclear Medicine and Biology, 2021, 92, 43-52.	0.6	1

#	Article	IF	CITATIONS
19	[18F]-JK-PSMA-7 PET/CT Under Androgen Deprivation Therapy in Advanced Prostate Cancer. Molecular Imaging and Biology, 2021, 23, 277-286.	2.6	8
20	On the consensus nomenclature rules for radiopharmaceutical chemistry – Reconsideration of radiochemical conversion. Nuclear Medicine and Biology, 2021, 93, 19-21.	0.6	43
21	Delivery of the Radionuclide 1311 Using Cationic Fusogenic Liposomes as Nanocarriers. International Journal of Molecular Sciences, 2021, 22, 457.	4.1	7
22	Rapid <sup>18</sup> F-labeling <i>via</i> Pd-catalyzed <i>S</i> arylation in aqueous medium. Chemical Communications, 2021, 57, 3547-3550.	4.1	7
23	<sup>18</sup> F-Labeled magnetic nanovectors for bimodal cellular imaging. Biomaterials Science, 2021, 9, 4717-4727.	5.4	6
24	Species Differences in Microsomal Metabolism of Xanthine-Derived A1 Adenosine Receptor Ligands. Pharmaceuticals, 2021, 14, 277.	3.8	1
25	Design, synthesis and biological evaluation of Tozadenant analogues as adenosine A2A receptor ligands. European Journal of Medicinal Chemistry, 2021, 214, 113214.	5.5	9
26	Towards chronic deep brain stimulation in freely moving hemiparkinsonian rats: applicability and functionality of a fully implantable stimulation system. Journal of Neural Engineering, 2021, 18, 036018.	3.5	1
27	Radiosynthesis and Biological Evaluation of [ <sup>18</sup> F]R91150, a Selective 5-HT <sub>2A</sub> Receptor Antagonist for PET-Imaging. ACS Medicinal Chemistry Letters, 2021, 12, 738-744.	2.8	4
28	Continuing Nuclear Data Research for Production of Accelerator-Based Novel Radionuclides for Medical Use: A Mini-Review. Frontiers in Physics, 2021, 9, .	2.1	17
29	Synthese und in vitro Evaluierung von F-18-markierten Adenosin-A1-Rezeptor Partialagonisten. Nuklearmedizin - NuclearMedicine, 2021, 60, .	0.7	0
30	Finding New Communities: A Principle of Neuronal Network Reorganization in Alzheimer's Disease. Brain Connectivity, 2021, 11, 225-238.	1.7	6
31	Binding characteristics of [ <sup>18</sup> F]PI-2620 distinguish the clinically predicted tau isoform in different tauopathies by PET. Journal of Cerebral Blood Flow and Metabolism, 2021, 41, 2957-2972.	4.3	30
32	Feasibility of short imaging protocols for [18F]PI-2620 tau-PET in progressive supranuclear palsy. European Journal of Nuclear Medicine and Molecular Imaging, 2021, 48, 3872-3885.	6.4	22
33	[ <sup>18</sup> F]ALX5406: A Brain-Penetrating Prodrug for GlyT1-Specific PET Imaging. ACS Chemical Neuroscience, 2021, 12, 3335-3346.	3.5	8
34	Drug Penetration into the Central Nervous System: Pharmacokinetic Concepts and In Vitro Model Systems. Pharmaceutics, 2021, 13, 1542.	4.5	18
35	Production of 6-l-[18F]Fluoro-m-tyrosine in an Automated Synthesis Module for 11C-Labeling. Molecules, 2021, 26, 5550.	3.8	2
36	Excitatory–inhibitory balance within EEG microstates and resting-state fMRI networks: assessed via simultaneous trimodal PET–MR–EEG imaging. Translational Psychiatry, 2021, 11, 60.	4.8	21

#	Article	IF	CITATIONS
37	Comparison of the Amyloid Load in the Brains of Two Transgenic Alzheimer's Disease Mouse Models Quantified by Florbetaben Positron Emission Tomography. Frontiers in Neuroscience, 2021, 15, 699926.	2.8	5
38	Production cross-section measurements of proton-induced reactions on natural tantalum in the 0.3â€ <sup>-</sup> GeV–1.7â€ <sup>-</sup> GeV energy range. Applied Radiation and Isotopes, 2021, 178, 109983.	1.5	0
39	Cerebral A1 adenosine receptor availability in female and male participants and its relationship to sleep. NeuroImage, 2021, 245, 118695.	4.2	8
40	Psilocybin targets a common molecular mechanism for cognitive impairment and increased craving in alcoholism. Science Advances, 2021, 7, eabh2399.	10.3	39
41	Evaluation of 3-l- and 3-d-[18F]Fluorophenylalanines as PET Tracers for Tumor Imaging. Cancers, 2021, 13, 6030.	3.7	4
42	Measurement of spallation cross sections for the production of terbium radioisotopes for medical applications from tantalum targets. Nuclear Instruments & Methods in Physics Research B, 2020, 463, 327-329.	1.4	5
43	Comparison of [18F]Fluoroethyltyrosine PET and Sodium MRI in Cerebral Gliomas: a Pilot Study. Molecular Imaging and Biology, 2020, 22, 198-207.	2.6	16
44	An <sup>18</sup> F-Labeled PSMA Ligand for PET/CT of Prostate Cancer: First-in-Humans Observational Study and Clinical Experience with <sup>18</sup> F-JK-PSMA-7 During the First Year of Application. Journal of Nuclear Medicine, 2020, 61, 202-209.	5.0	23
45	Intraindividual Comparison of <sup>18</sup> F-PSMA-1007 with Renally Excreted PSMA Ligands for PSMA PET Imaging in Patients with Relapsed Prostate Cancer. Journal of Nuclear Medicine, 2020, 61, 729-734.	5.0	58
46	Influence of binding affinity and blood plasma level on cerebral pharmacokinetics and PET imaging characteristics of two novel xanthine PET radioligands for the A1 adenosine receptor. Nuclear Medicine and Biology, 2020, 82-83, 1-8.	0.6	1
47	Bolus infusion scheme for the adjustment of steady state [11C]Flumazenil levels in the grey matter and in the blood plasma for neuroreceptor imaging. NeuroImage, 2020, 221, 117160.	4.2	2
48	Preparation of 5-[131I]iodotubercidin for the detection of adenosine kinase. Journal of Radioanalytical and Nuclear Chemistry, 2020, 326, 1691-1697.	1.5	0
49	Entorhinal Tau Predicts Hippocampal Activation and Memory Deficits in Alzheimer's Disease. Journal of Alzheimer's Disease, 2020, 78, 1601-1614.	2.6	5
50	Development and Evaluation of a Versatile Receptor-Ligand Binding Assay Using Cell Membrane Preparations Embedded in an Agarose Gel Matrix and Evaluation with the Human Adenosine A1Receptor. Assay and Drug Development Technologies, 2020, 18, 328-340.	1.2	1
51	Dnmt3a2/Dnmt3L Overexpression in the Dopaminergic System of Mice Increases Exercise Behavior through Signaling Changes in the Hypothalamus. International Journal of Molecular Sciences, 2020, 21, 6297.	4.1	6
52	Assessment of <sup>18</sup> F-PI-2620 as a Biomarker in Progressive Supranuclear Palsy. JAMA Neurology, 2020, 77, 1408.	9.0	145
53	ADORA2A variation and adenosine A1 receptor availability in the human brain with a focus on anxiety-related brain regions: modulation by ADORA1 variation. Translational Psychiatry, 2020, 10, 406.	4.8	15
54	Nuclear Medicine in Times of COVID-19: How Radiopharmaceuticals Could Help to Fight the Current and Future Pandemics. Pharmaceutics, 2020, 12, 1247.	4.5	10

#	Article	IF	CITATIONS
55	Investigation of Cerebral O-(2-[18F]Fluoroethyl)-L-Tyrosine Uptake in Rat Epilepsy Models. Molecular Imaging and Biology, 2020, 22, 1255-1265.	2.6	3
56	mGluR5 receptor availability is associated with lower levels of negative symptoms and better cognition in male patients with chronic schizophrenia. Human Brain Mapping, 2020, 41, 2762-2781.	3.6	20
57	Preparation of labeled aromatic amino acids via late-stage 18F-fluorination of chiral nickel and copper complexes. Chemical Communications, 2020, 56, 9505-9508.	4.1	10
58	Preparation of a First 18F-Labeled Agonist for M1 Muscarinic Acetylcholine Receptors. Molecules, 2020, 25, 2880.	3.8	8
59	Prediction of survival in patients with IDH-wildtype astrocytic gliomas using dynamic O-(2-[18F]-fluoroethyl)-l-tyrosine PET. European Journal of Nuclear Medicine and Molecular Imaging, 2020, 47, 1486-1495.	6.4	16
60	Flare Phenomenon in O-(2-18F-Fluoroethyl)-l-Tyrosine PET After Resection of Gliomas. Journal of Nuclear Medicine, 2020, 61, 1294-1299.	5.0	10
61	High uptake of 68Ga-PSMA and 18F-DCFPyL in the peritumoral area of rat gliomas due to activated astrocytes. EJNMMI Research, 2020, 10, 55.	2.5	13
62	Accurate determination of production data of the non-standard positron emitter <sup>86</sup> Y via the <sup>86</sup> Sr(p,n)-reaction. Radiochimica Acta, 2020, 108, 747-756.	1.2	14
63	Positron-Emission-Tomography Imaging of Long-Term Expression of the 18kDa Translocator Protein After Sudden Cardiac Arrest in Rats. Shock, 2020, Publish Ahead of Print, 620-629.	2.1	4
64	11C- and 18F-labelled tryptophans as PET-tracers for imaging of altered tryptophan metabolism in age-associated disorders. Russian Chemical Reviews, 2020, 89, 879-896.	6.5	4
65	Radiopharmaceutical Sciences. , 2020, , 49-191.		2
66	Influence of Dexamethasone on O-(2-[18F]-Fluoroethyl)-l-Tyrosine Uptake in the Human Brain and Quantification of Tumor Uptake. Molecular Imaging and Biology, 2019, 21, 168-174.	2.6	11
67	Spatial distributions of cholinergic impairment and neuronal hypometabolism differ in MCI due to AD. NeuroImage: Clinical, 2019, 24, 101978.	2.7	11
68	Biodistribution and radiation dosimetry of [18F]-JK-PSMA-7 as a novel prostate-specific membrane antigen-specific ligand for PET/CT imaging of prostate cancer. EJNMMI Research, 2019, 9, 66.	2.5	24
69	Peripheral ganglia in healthy rats as target structures for the evaluation of PSMA imaging agents. BMC Cancer, 2019, 19, 633.	2.6	5
70	Positron-emitting radionuclides for applications, with special emphasis on their production methodologies for medical use. Radiochimica Acta, 2019, 107, 1011-1026.	1.2	22
71	Alcohol-Supported Cu-Mediated 18F-Fluorination of Iodonium Salts under "Minimalist―Conditions. Molecules, 2019, 24, 3197.	3.8	13
72	Level of education mitigates the impact of tau pathology on neuronal function. European Journal of Nuclear Medicine and Molecular Imaging, 2019, 46, 1787-1795.	6.4	16

#	Article	IF	CITATIONS
73	Minimalist approach meets green chemistry: Synthesis of <sup>18</sup> F―labeled (hetero)aromatics in pure ethanol. Journal of Labelled Compounds and Radiopharmaceuticals, 2019, 62, 404-410.	1.0	11
74	Effects of subthalamic deep brain stimulation on striatal metabolic connectivity in a rat hemiparkinsonian model. DMM Disease Models and Mechanisms, 2019, 12, .	2.4	8
75	Baeyerâ€Villiger oxidation tuned to chemoselective conversion of nonâ€activated [ <sup>18</sup> F]fluorobenzaldehydes to [ <sup>18</sup> F]fluorophenols. Journal of Labelled Compounds and Radiopharmaceuticals, 2019, 62, 380-392.	1.0	2
76	Relevance of In Vitro Metabolism Models to PET Radiotracer Development: Prediction of In Vivo Clearance in Rats from Microsomal Stability Data. Pharmaceuticals, 2019, 12, 57.	3.8	10
77	<sup>52g/55</sup> Mn-Labelled CDTA-based trimeric complexes as novel bimodal PET/MR probes with high relaxivity. Dalton Transactions, 2019, 48, 3003-3008.	3.3	6
78	Discovery of <sup>18</sup> F-JK-PSMA-7, a PET Probe for the Detection of Small PSMA-Positive Lesions. Journal of Nuclear Medicine, 2019, 60, 817-823.	5.0	41
79	Influence of incubation conditions on microsomal metabolism of xanthine-derived A1 adenosine receptor ligands. Journal of Pharmacological and Toxicological Methods, 2019, 95, 16-26.	0.7	6
80	Simultaneous PET-MR-EEC: Technology, Challenges and Application in Clinical Neuroscience. IEEE Transactions on Radiation and Plasma Medical Sciences, 2019, 3, 377-385.	3.7	9
81	2-[18F]Fluorophenylalanine: Synthesis by Nucleophilic 18F-Fluorination and Preliminary Biological Evaluation. Synthesis, 2019, 51, 664-676.	2.3	12
82	FET PET reveals considerable spatial differences in tumour burden compared to conventional MRI in newly diagnosed glioblastoma. European Journal of Nuclear Medicine and Molecular Imaging, 2019, 46, 591-602.	6.4	74
83	Discovery of F-18-JK-PSMA-7 as PET-probe suitable for imaging of small PSMA expressing lesions. Nuklearmedizin - NuclearMedicine, 2019, 58, .	0.7	2
84	FET PET reveals considerable spatial differences in tumour burden compared to conventional MRI in newly diagnosed glioblastoma. Nuklearmedizin - NuclearMedicine, 2019, 58, .	0.7	0
85	Comparison of [18F]-Fluoroethyltyrosine PET and the IDH status with Sodium MRI in Cerebral Gliomas. , 2019, 58, .		Ο
86	Combined FET PET/MRI radiomics differentiates radiation injury from recurrent brain metastasis. , 2019, 58, .		0
87	Investigation of cis-4-[18F]Fluoro-D-Proline Uptake in Human Brain Tumors After Multimodal Treatment. Molecular Imaging and Biology, 2018, 20, 1035-1043.	2.6	6
88	Heinz H. Coenen—A pioneer in the field of nuclear and radiochemistry. Journal of Labelled Compounds and Radiopharmaceuticals, 2018, 61, 122-123.	1.0	0
89	Networks of tau distribution in Alzheimer's disease. Brain, 2018, 141, 568-581.	7.6	140
90	Effect of cholinergic treatment depends on cholinergic integrity in early Alzheimer's disease. Brain, 2018, 141, 903-915.	7.6	65

#	Article	IF	CITATIONS
91	lsolation of high purity <sup>73</sup> Se using solid phase extraction after selective 4,5-[ <sup>73</sup> Se]benzopiazselenol formation with aminonaphthalene. Radiochimica Acta, 2018, 106, 497-505.	1.2	5
92	Discovery of 7-[ <sup>18</sup> F]Fluorotryptophan as a Novel Positron Emission Tomography (PET) Probe for the Visualization of Tryptophan Metabolism in Vivo. Journal of Medicinal Chemistry, 2018, 61, 189-206.	6.4	61
93	Static and dynamic 18F–FET PET for the characterization of gliomas defined by IDH and 1p/19q status. European Journal of Nuclear Medicine and Molecular Imaging, 2018, 45, 443-451.	6.4	95
94	P05.11 Combined FET PET/MRI radiomics for the differentiation of radiation injury from recurrent brain metastasis. Neuro-Oncology, 2018, 20, iii304-iii304.	1.2	0
95	P1â€458: LEVEL OF BRAIN RESERVE ASSOCIATED WITH SPATIAL EXTENT OF TAUâ€NEURODEGENERATION PATTE IN ALZHEIMER'S DISEASE. Alzheimer's and Dementia, 2018, 14, P494.	IRN 0.8	0
96	Uptake in non-affected bone tissue does not differ between [18F]-DCFPyL and [68Ga]-HBED-CC PSMA PET/CT. PLoS ONE, 2018, 13, e0209613.	2.5	9
97	Role of Extracellular Loops and Membrane Lipids for Ligand Recognition in the Neuronal Adenosine Receptor Type 2A: An Enhanced Sampling Simulation Study. Molecules, 2018, 23, 2616.	3.8	13
98	New developments in the production of theranostic pairs of radionuclides. Journal of Radioanalytical and Nuclear Chemistry, 2018, 318, 1493-1509.	1.5	112
99	Structural Prediction of the Dimeric Form of the Mammalian Translocator Membrane Protein TSPO: A Key Target for Brain Diagnostics. International Journal of Molecular Sciences, 2018, 19, 2588.	4.1	15
100	Predicting IDH genotype in gliomas using FET PET radiomics. Scientific Reports, 2018, 8, 13328.	3.3	90
101	18F-labelling innovations and their potential for clinical application. Clinical and Translational Imaging, 2018, 6, 169-193.	2.1	37
102	In vivo Molecular Imaging of Clutamate Carboxypeptidase II Expression in Re-endothelialisation after Percutaneous Balloon Denudation in a Rat Model. Scientific Reports, 2018, 8, 7411.	3.3	5
103	Combined FET PET/MRI radiomics differentiates radiation injury from recurrent brain metastasis. NeuroImage: Clinical, 2018, 20, 537-542.	2.7	113
104	Diagnostic potential of PET/CT using a 68Ga-labelled prostate-specific membrane antigen ligand in whole-body staging of renal cell carcinoma: initial experience. European Journal of Nuclear Medicine and Molecular Imaging, 2017, 44, 102-107.	6.4	87
105	White matter lesions and the cholinergic deficit in aging and mild cognitive impairment. Neurobiology of Aging, 2017, 53, 27-35.	3.1	36
106	Novel ion exchange chromatography method for nca arsenic separation. Applied Radiation and Isotopes, 2017, 122, 111-115.	1.5	11
107	Synthesis and Pharmacological Evaluation of Identified and Putative Metabolites of the A <sub>1</sub> Adenosine Receptor Antagonist 8 yclopentylâ€3â€{3â€fluoropropyl)â€1â€propylxanthine (CPFPX). ChemMed 2017, 12, 770-784.	Chem,	3
108	Influence of Bevacizumab on Blood–Brain Barrier Permeability and <i>O</i> -(2- <sup>18</sup> F-Fluoroethyl)-l-Tyrosine Uptake in Rat Gliomas. Journal of Nuclear Medicine, 2017, 58, 700-705.	5.0	27

#	Article	IF	CITATIONS
109	Imaging of amino acid transport in brain tumours: Positron emission tomography with O-(2-[18) Tj ETQq1 1 0.78	4314 rgBT	Qverlock
110	PSA-Stratified Performance of <sup>18</sup> F- and <sup>68</sup> Ga-PSMA PET in Patients with Biochemical Recurrence of Prostate Cancer. Journal of Nuclear Medicine, 2017, 58, 947-952.	5.0	150
111	Alcoholâ€Enhanced Cuâ€Mediated Radiofluorination. Chemistry - A European Journal, 2017, 23, 3251-3256.	3.3	104
112	Production of medically useful bromine isotopes via alpha-particle induced nuclear reactions. EPJ Web of Conferences, 2017, 146, 08006.	0.3	1
113	[P2–200]: <i>IN VIVO</i> TAUOPATHY MEASURED WITH [18F]â€AVâ€1451 IS DIFFERENTIALLY RELATED TO C BIOMARKERS OF TAU IN ALZHEIMER'S DISEASE: THE INFLUENCE OF AMYLOID DEPOSITION. Alzheimer's and Dementia, 2017, 13, P683.	SF 0.8	Ο
114	New irradiation facilities for development of production methods of medical radionuclides at cyclotrons at Forschungszentrum JÃ1/4lich. , 2017, , .		1
115	Novel CDTA-based, Bifunctional Chelators for Stable and Inert Mn <sup>II</sup> Complexation: Synthesis and Physicochemical Characterization. Inorganic Chemistry, 2017, 56, 7746-7760.	4.0	36
116	Radiation injury vs. recurrent brain metastasis: combining textural feature radiomics analysis and standard parameters may increase 18F-FET PET accuracy without dynamic scans. European Radiology, 2017, 27, 2916-2927.	4.5	81
117	Influence of blood-brain barrier permeability on O-(2-18F-fluoroethyl)-L-tyrosine uptake in rat gliomas. European Journal of Nuclear Medicine and Molecular Imaging, 2017, 44, 408-416.	6.4	21
118	A Practical Method for the Preparation of 18F-Labeled Aromatic Amino Acids from Nucleophilic [18F]Fluoride and Stannyl Precursors for Electrophilic Radiohalogenation. Molecules, 2017, 22, 2231.	3.8	30
119	Motor impairment and compensation in a hemiparkinsonian rat model: correlation between dopamine depletion severity, cerebral metabolism and gait patterns. EJNMMI Research, 2017, 7, 68.	2.5	14
120	Convenient Preparation of 18F-Labeled Peptide Probes for Potential Claudin-4 PET Imaging. Pharmaceuticals, 2017, 10, 99.	3.8	10
121	Radioiodinated indomethacin amide for molecular imaging of cyclooxygenase-2 expressing tumors. Oncotarget, 2017, 8, 18059-18069.	1.8	5
122	Imaging in Neurology Research III: Neurodegenerative Diseases. , 2017, , 761-772.		0
123	The Functional Networks of Prepulse Inhibition: Neuronal Connectivity Analysis Based on FDG-PET in Awake and Unrestrained Rats. Frontiers in Behavioral Neuroscience, 2016, 10, 148.	2.0	47
124	Seyferth–Gilbert Homologation as a Route to <sup>18</sup> F‣abeled Building Blocks: Preparation of RadiofluorÂinated Phenylacetylenes and Their Application in PET Chemistry. European Journal of Organic Chemistry, 2016, 2016, 430-433.	2.4	10
125	The use ofO-(2-18F-fluoroethyl)-L-tyrosine PET in the diagnosis of gliomas located in the brainstem and spinal cord. Neuro-Oncology, 2016, 19, now243.	1.2	8
126	In vivo Patterns of Tau Pathology, Amyloid-β Burden, and Neuronal Dysfunction in Clinical Variants of Alzheimer's Disease. Journal of Alzheimer's Disease, 2016, 55, 465-471.	2.6	93

#	Article	IF	CITATIONS
127	Impact of tau and amyloid burden on glucose metabolism in Alzheimer's disease. Annals of Clinical and Translational Neurology, 2016, 3, 934-939.	3.7	89
128	Transcranial direct current stimulation accelerates recovery of function, induces neurogenesis and recruits oligodendrocyte precursors in a rat model of stroke. Experimental Neurology, 2016, 279, 127-136.	4.1	77
129	Glucose consumption of inflammatory cells masks metabolic deficits in the brain. NeuroImage, 2016, 128, 54-62.	4.2	52
130	Prostate-Specific Membrane Antigen–Targeted Radiohalogenated PET and Therapeutic Agents for Prostate Cancer. Journal of Nuclear Medicine, 2016, 57, 90S-96S.	5.0	48
131	Preparation of Noâ€Carrierâ€Added 6â€{ <sup>18</sup> F]Fluoroâ€ <scp>l</scp> â€tryptophan via Cuâ€Mediated Radiofluorination. European Journal of Organic Chemistry, 2016, 2016, 4621-4628.	2.4	26
132	Circadian variation of metabotropic glutamate receptor 5 availability in the rat brain. Journal of Sleep Research, 2016, 25, 754-761.	3.2	47
133	Automated synthesis of 4-[18F]fluoroanisole, [18F]DAA1106 and 4-[18F]FPhe using Cu-mediated radiofluorination under "minimalist―conditions. Applied Radiation and Isotopes, 2016, 115, 133-137.	1.5	26
134	D26â€Pathological tau signal in huntington's disease – an in vivo [18F]-AV-1451 pet imaging report. Journal of Neurology, Neurosurgery and Psychiatry, 2016, 87, A44.1-A44.	1.9	2
135	Uses of alpha particles, especially in nuclear reaction studies and medical radionuclide production. Radiochimica Acta, 2016, 104, 601-624.	1.2	52
136	The Neural Cell Adhesion Molecule-Derived (NCAM)-Peptide FG Loop (FGL) Mobilizes Endogenous Neural Stem Cells and Promotes Endogenous Regenerative Capacity after Stroke. Journal of NeuroImmune Pharmacology, 2016, 11, 708-720.	4.1	17
137	Radiolabelling with isotopic mixtures of <sup>52g/55</sup> Mn( <scp>ii</scp> ) as a straight route to stable manganese complexes for bimodal PET/MR imaging. Dalton Transactions, 2016, 45, 1315-1321.	3.3	22
138	A Practical Oneâ€Pot Synthesis of Positron Emission Tomography (PET) Tracers via Nickelâ€Mediated Radiofluorination. ChemistryOpen, 2015, 4, 457-462.	1.9	30
139	A Practical One-Pot Synthesis of Positron Emission Tomography (PET) Tracers via Nickel-Mediated Radiofluorination. ChemistryOpen, 2015, 4, 395-395.	1.9	0
140	A threeâ€step radiosynthesis of 6â€{ <sup>18</sup> F]fluoroâ€ <i>Lâ€meta</i> â€tyrosine starting with [ <sup>18</sup> F]fluoride. Journal of Labelled Compounds and Radiopharmaceuticals, 2015, 58, 133-140.	1.0	7
141	4-[18F]Fluorophenylpiperazines by Improved Hartwig-Buchwald N-Arylation of 4-[18F]fluoroiodobenzene, Formed via Hypervalent I»3-Iodane Precursors: Application to Build-Up of the Dopamine D4 Ligand [18F]FAUC 316. Molecules, 2015, 20, 470-486.	3.8	21
142	Authentically radiolabelled Mn(II) complexes as bimodal PET/MR tracers. EJNMMI Physics, 2015, 2, A85.	2.7	3
143	Longitudinal assessment of infarct progression, brain metabolism and behavior following anterior cerebral artery occlusion in rats. Journal of Neuroscience Methods, 2015, 253, 279-291.	2.5	9
144	Comparison of [18F]DCFPyL and [68Ga]Ga-PSMA-HBED-CC for PSMA-PET Imaging in Patients with Relapsed Prostate Cancer. Molecular Imaging and Biology, 2015, 17, 575-584.	2.6	288

#	Article	IF	CITATIONS
145	In vivo analysis of neuroinflammation in the late chronic phase after experimental stroke. Neuroscience, 2015, 292, 71-80.	2.3	49
146	Copperâ€Mediated Aromatic Radiofluorination Revisited: Efficient Production of PET Tracers on a Preparative Scale. Chemistry - A European Journal, 2015, 21, 5972-5979.	3.3	113
147	Radiosynthesis of 4-[ 18 F]fluoro- l -tryptophan by isotopic exchange on carbonyl-activated precursors. Bioorganic and Medicinal Chemistry, 2015, 23, 5856-5869.	3.0	14
148	Intermittent high-dose treatment with erlotinib enhances therapeutic efficacy in EGFR-mutant lung cancer. Oncotarget, 2015, 6, 38458-38468.	1.8	19
149	Developments in oncological positron emission tomography/computed tomography assessment. Journal of Thoracic Disease, 2015, 7, E637-9.	1.4	0
150	Recent Trends in Pharmaceutical Radiochemistry for Molecular PET Imaging. BioMed Research International, 2014, 2014, 1-3.	1.9	1
151	Aromatic-turmerone induces neural stem cell proliferation in vitro and in vivo. Stem Cell Research and Therapy, 2014, 5, 100.	5.5	69
152	Nondestructive monitoring of tissue-engineered constructs. Biomedizinische Technik, 2014, 59, 165-75.	0.8	8
153	Optimizing the transfer of [18F]fluoride from aqueous to organic solvents by electrodeposition using carbon electrodes. Applied Radiation and Isotopes, 2014, 91, 1-7.	1.5	5
154	Acute and Sustained Effects of Methylphenidate on Cognition and Presynaptic Dopamine Metabolism: An [ <sup>18</sup> F]FDOPA PET Study. Journal of Neuroscience, 2014, 34, 14769-14776.	3.6	24
155	Neither azeotropic drying, nor base nor other additives: a minimalist approach to <sup>18</sup> F-labeling. Organic and Biomolecular Chemistry, 2014, 12, 8094-8099.	2.8	86
156	lodonium ylides for one-step, no-carrier-added radiofluorination of electron rich arenes, exemplified with 4-(([18F]fluorophenoxy)-phenylmethyl)piperidine NET and SERT ligands. RSC Advances, 2014, 4, 17293-17299.	3.6	70
157	Transient Antiangiogenic Treatment Improves Delivery of Cytotoxic Compounds and Therapeutic Outcome in Lung Cancer. Cancer Research, 2014, 74, 2816-2824.	0.9	26
158	The integrity of the cholinergic system determines memory performance in healthy elderly. NeuroImage, 2014, 100, 481-488.	4.2	30
159	Towards authentically labelled bi-modal PET(SPECT)/MR-probes. EJNMMI Physics, 2014, 1, A79.	2.7	5
160	The synthetic NCAM mimetic peptide FGL mobilizes neural stem cells in vitro and in vivo. Stem Cell Reviews and Reports, 2014, 10, 539-547.	5.6	18
161	Synthesis of <sup>18</sup> Fâ€Labelled βâ€Lactams by Using the Kinugasa Reaction. Chemistry - A European Journal, 2014, 20, 4697-4703.	3.3	24
162	In-vivo detection of inflammation and neurodegeneration in the chronic phase after permanent embolic stroke in rats. Brain Research, 2014, 1581, 80-88.	2.2	43

#	Article	IF	CITATIONS
163	Neural correlates of sensorimotor gating: a metabolic positron emission tomography study in awake rats. Frontiers in Behavioral Neuroscience, 2014, 8, 178.	2.0	21
164	Non-invasive imaging of glioma vessel size and densities in correlation with tumour cell proliferation by small animal PET and MRI. European Journal of Nuclear Medicine and Molecular Imaging, 2013, 40, 1595-1606.	6.4	15
165	Imaging microglial activation and glucose consumption in a mouse model of Alzheimer's disease. Neurobiology of Aging, 2013, 34, 351-354.	3.1	52
166	Tumor VEGF:VEGFR2 autocrine feed-forward loop triggers angiogenesis in lung cancer. Journal of Clinical Investigation, 2013, 123, 1732-1740.	8.2	166
167	Tumor VEGF:VEGFR2 autocrine feed-forward loop triggers angiogenesis in lung cancer. Journal of Clinical Investigation, 2013, 123, 3183-3183.	8.2	7
168	Prognostic Impact of [18F]Fluorothymidine and [18F]Fluoro-D-Glucose Baseline Uptakes in Patients with Lung Cancer Treated First-Line with Erlotinib. PLoS ONE, 2013, 8, e53081.	2.5	36
169	Analysis of the Growth Dynamics of Angiogenesis-Dependent and -Independent Experimental Glioblastomas by Multimodal Small-Animal PET and MRI. Journal of Nuclear Medicine, 2012, 53, 1135-1145.	5.0	38
170	Potential of Early [ <sup>18</sup> F]-2-Fluoro-2-Deoxy-D-Glucose Positron Emission Tomography for Identifying Hypoperfusion and Predicting Fate of Tissue in a Rat Embolic Stroke Model. Stroke, 2012, 43, 193-198.	2.0	32
171	Tumor Lesion Glycolysis and Tumor Lesion Proliferation for Response Prediction and Prognostic Differentiation in Patients With Advanced Non–Small Cell Lung Cancer Treated With Erlotinib. Clinical Nuclear Medicine, 2012, 37, 1058-1064.	1.3	47
172	Carrierâ€effect on palladiumâ€catalyzed, nucleophilic <sup>18</sup> Fâ€fluorination of aryl triflates. Journal of Labelled Compounds and Radiopharmaceuticals, 2012, 55, 450-453.	1.0	19
173	Beyond azide–alkyne click reaction: easy access to 18F-labelled compounds via nitrile oxide cycloadditions. Chemical Communications, 2012, 48, 7134.	4.1	30
174	Cholinergic system function and cognition in mild cognitive impairment. Neurobiology of Aging, 2012, 33, 867-877.	3.1	96
175	Effects of minocycline on endogenous neural stem cells after experimental stroke. Neuroscience, 2012, 215, 174-183.	2.3	47
176	Monitoring reversible and irreversible EGFR inhibition with erlotinib and afatinib in a patient with EGFR-mutated non-small cell lung cancer (NSCLC) using sequential [18F]fluorothymidine (FLT-)PET. Lung Cancer, 2012, 77, 617-620.	2.0	14
177	The Bioenergetic Status Relates to Dopamine Neuron Loss in Familial PD with PINK1 Mutations. PLoS ONE, 2012, 7, e51308.	2.5	13
178	Conflict Processing in the Rat Brain: Behavioral Analysis and Functional μPET Imaging Using [18F]Fluorodeoxyglucose. Frontiers in Behavioral Neuroscience, 2012, 6, 4.	2.0	15
179	Predictive value of early and late residual 18F-fluorodeoxyglucose and 18F-fluorothymidine uptake using different SUV measurements in patients with non-small-cell lung cancer treated with erlotinib. European Journal of Nuclear Medicine and Molecular Imaging, 2012, 39, 1117-1127.	6.4	43
180	C-(4-[18F]fluorophenyl)-N-phenyl nitrone: A novel 18F-labeled building block for metal free [3+2]cycloaddition. Applied Radiation and Isotopes, 2012, 70, 184-192.	1.5	16

#	Article	IF	CITATIONS
181	Evaluation of18F-Labeled Benzodioxine Piperazine-Based Dopamine D4Receptor Ligands: Lipophilicity as a Determinate of Nonspecific Binding. Journal of Medicinal Chemistry, 2011, 54, 8343-8352.	6.4	26
182	Early Prediction of Nonprogression in Advanced Non–Small-Cell Lung Cancer Treated With Erlotinib By Using [ <sup>18</sup> F]Fluorodeoxyglucose and [ <sup>18</sup> F]Fluorothymidine Positron Emission Tomography. Journal of Clinical Oncology, 2011, 29, 1701-1708.	1.6	170
183	Tc-99m-MIBI-Negative Parathyroid Adenoma in Primary Hyperparathyroidism Detected by C-11-Methionine PET/CT After Previous Thyroid Surgery. Clinical Nuclear Medicine, 2011, 36, 1153-1155.	1.3	10
184	Whiskers Area as Extracerebral Reference Tissue for Quantification of Rat Brain Metabolism Using <sup>18</sup> F-FDG PET: Application to Focal Cerebral Ischemia. Journal of Nuclear Medicine, 2011, 52, 1252-1260.	5.0	33
185	Quantitative Analysis of Response to Treatment with Erlotinib in Advanced Non–Small Cell Lung Cancer Using 18F-FDG and 3′-Deoxy-3′-18F-Fluorothymidine PET. Journal of Nuclear Medicine, 2011, 52, 1871-1877.	5.0	65
186	Clinical value of 18F-fluorodihydroxyphenylalanine positron emission tomography/computed tomography (18F-DOPA PET/CT) for detecting pheochromocytoma. European Journal of Nuclear Medicine and Molecular Imaging, 2010, 37, 484-493.	6.4	62
187	Synthesis and evaluation of 18F-fluoroethylated benzothiazole derivatives for in vivo imaging of amyloid plaques in Alzheimer's disease. Applied Radiation and Isotopes, 2010, 68, 1066-1072.	1.5	15
188	Progression of subtle motor signs in <i>PINK1</i> mutation carriers with mild dopaminergic deficit. Neurology, 2010, 74, 1798-1805.	1.1	60
189	Clinical Value of 18-Fluorine-Fluorodihydroxyphenylalanine Positron Emission Tomography/Computed Tomography in the Follow-Up of Medullary Thyroid Carcinoma. Thyroid, 2010, 20, 527-533.	4.5	78
190	Noninvasive Imaging of Endogenous Neural Stem Cell Mobilization <i>In Vivo</i> Using Positron Emission Tomography. Journal of Neuroscience, 2010, 30, 6454-6460.	3.6	97
191	Three-Step, "One-Pot―Radiosynthesis of 6-Fluoro-3,4-Dihydroxy-l-Phenylalanine by Isotopic Exchange. Journal of Nuclear Medicine, 2009, 50, 1724-1729.	5.0	63
192	Synthesis, radiofluorination and first evaluation of (±)â€[ <sup>18</sup> F]MDL 100907 as serotonin 5â€HT <sub>2A</sub> receptor antagonist for PET. Journal of Labelled Compounds and Radiopharmaceuticals, 2009, 52, 6-12.	1.0	23
193	Synthesis, labelling and first evaluation of [ <sup>18</sup> F]R91150 as a serotonin 5â€HT <sub>2A</sub> receptor antagonist for PET. Journal of Labelled Compounds and Radiopharmaceuticals, 2009, 52, 13-22.	1.0	18
194	Noninvasive quantification of 18F-FLT human brain PET for the assessment of tumour proliferation in patients with high-grade glioma. European Journal of Nuclear Medicine and Molecular Imaging, 2009, 36, 1960-1967.	6.4	59
195	Neuroinflammation Extends Brain Tissue at Risk to Vital Peri-Infarct Tissue: A Double Tracer [ <sup>11</sup> C]PK11195- and [ <sup>18</sup> F]FDG-PET Study. Journal of Cerebral Blood Flow and Metabolism, 2009, 29, 1216-1225.	4.3	114
196	A fully automated two-step synthesis of an 18F-labelled tyrosine kinase inhibitor for EGFR kinase activity imaging in tumors. Applied Radiation and Isotopes, 2009, 67, 1977-1984.	1.5	27
197	<i>Short Communication:</i> <sup>18</sup> F-Immuno-PET: Determination of Anti-CD66 Biodistribution in a Patient with High-Risk Leukemia. Cancer Biotherapy and Radiopharmaceuticals, 2008, 23, 819-824.	1.0	14
198	Glioma Proliferation as Assessed by 3â€~-Fluoro-3'-Deoxy- <scp>l</scp> -Thymidine Positron Emission Tomography in Patients with Newly Diagnosed High-Grade Glioma. Clinical Cancer Research, 2008, 14, 2049-2055.	7.0	129

#	Article	IF	CITATIONS
199	Early Detection of Erlotinib Treatment Response in NSCLC by 3′-Deoxy-3′-[18F]-Fluoro-L-Thymidine ([18F]FLT) Positron Emission Tomography (PET). PLoS ONE, 2008, 3, e3908.	2.5	80
200	Sleep Deprivation Increases A1 Adenosine Receptor Binding in the Human Brain: A Positron Emission Tomography Study. Journal of Neuroscience, 2007, 27, 2410-2415.	3.6	169
201	Labelling of a monoclonal antibody with 68Ga using three DTPA-based bifunctional ligands and their in vitro evaluation for application in radioimmunotherapy. Radiochimica Acta, 2007, 95, 39-42.	1.2	16
202	Synthesis and biodistribution of 3′-fluoro-5-[1311]iodo-2′-deoxyuridine: a comparative study of [1311]FLIdU and [18F]FLT. Nuclear Medicine and Biology, 2007, 34, 273-281.	0.6	1
203	Nucleophilic18F-Fluorination of Heteroaromatic Iodonium Salts with No-Carrier-Added [18F]Fluoride. Journal of the American Chemical Society, 2007, 129, 8018-8025.	13.7	194
204	Direct comparison of [18F]FDG PET/CT with PET alone and with side-by-side PET and CT in patients with malignant melanoma. European Journal of Nuclear Medicine and Molecular Imaging, 2007, 34, 1355-1364.	6.4	53
205	Early assessment of therapy response in malignant lymphoma with the thymidine analogue [18F]FLT. European Journal of Nuclear Medicine and Molecular Imaging, 2007, 34, 1775-1782.	6.4	62
206	Radiosynthesis and evaluation of [11C]BTA-1 and [11C]3'-Me-BTA-1 as potential radiotracers for in vivo imaging of-amyloid plaques. Nuklearmedizin - NuclearMedicine, 2007, , .	0.7	1
207	Synthesis and evaluation of a radiometal-labeled macrocyclic chelator-derivatised thymidine analog. Nuclear Medicine and Biology, 2006, 33, 359-366.	0.6	19
208	Molecular Imaging of Proliferation in Malignant Lymphoma. Cancer Research, 2006, 66, 11055-11061.	0.9	173
209	188Re or 90Y-labelled anti-CD66 antibody as part of a dose-reduced conditioning regimen for patients with acute leukaemia or myelodysplastic syndrome over the age of 55: results of a phase I-II study. British Journal of Haematology, 2005, 130, 604-613.	2.5	92
210	Clinical relevance of imaging proliferative activity in lung nodules. European Journal of Nuclear Medicine and Molecular Imaging, 2005, 32, 525-533.	6.4	101
211	Lymph Node Staging in Lung Cancer Using [18F]FDG-PET. Thoracic and Cardiovascular Surgeon, 2004, 52, 96-101.	1.0	35
212	[ 18 F] 3-deoxy-3′-fluorothymidine positron emission tomography: alternative or diagnostic adjunct to 2-[ 18 f]-fluoro-2-deoxy- d -glucose positron emission tomography in the workup of suspicious central focal lesions?. Journal of Thoracic and Cardiovascular Surgery, 2004, 127, 1093-1099.	0.8	33
213	Imaging of activated microglia with PET and [11 C]PK 11195 in corticobasal degeneration. Movement Disorders, 2004, 19, 817-821.	3.9	39
214	[18F]3'-Deoxy-3'-Fluorothymidine-PET in NHL Patients: Whole-Body Biodistribution and Imaging of Lymphoma Manifestations—a Pilot Study. Cancer Biotherapy and Radiopharmaceuticals, 2004, 19, 436-442.	1.0	12
215	[ <sup>18</sup> F]3′-Deoxy-3′-Fluorothymidine–PET in NHL Patients: Whole-Body Biodistribution and Imaging of Lymphoma Manifestations—a Pilot Study. Cancer Biotherapy and Radiopharmaceuticals, 2004, 19, 436-442.	1.0	37
216	3'-[18F]fluoro-3'-deoxythymidine ([18F]-FLT) as positron emission tomography tracer for imaging proliferation in a murine B-Cell lymphoma model and in the human disease. Cancer Research, 2003, 63, 2681-7.	0.9	128

#	Article	IF	CITATIONS
217	Imaging proliferation in lung tumors with PET: 18F-FLT versus 18F-FDG. Journal of Nuclear Medicine, 2003, 44, 1426-31.	5.0	281
218	Evaluation of pyrimidine metabolising enzymes and in vitro uptake of 3'-[18F]fluoro-3'-deoxythymidine ([18F]FLT) in pancreatic cancer cell lines. European Journal of Nuclear Medicine and Molecular Imaging, 2002, 29, 1174-1181.	6.4	70
219	Carbon-11 acetate positron emission tomography can detect local recurrence of prostate cancer. European Journal of Nuclear Medicine and Molecular Imaging, 2002, 29, 1380-1384.	6.4	144
220	3-deoxy-3-[(18)F]fluorothymidine-positron emission tomography for noninvasive assessment of proliferation in pulmonary nodules. Cancer Research, 2002, 62, 3331-4.	0.9	162
221	Targeted bone marrow irradiation in the conditioning of high-risk leukaemia prior to stem cell transplantation. European Journal of Nuclear Medicine and Molecular Imaging, 2001, 28, 807-815.	2.1	36
222	Validation of myocardial blood flow estimation with nitrogen-13 ammonia PET by the argon inert gas technique in humans. European Journal of Nuclear Medicine and Molecular Imaging, 2001, 28, 340-345.	2.1	13
223	In vivo imaging of activated microglia using [11 C]PK11195 and positron emission tomography in patients after ischemic stroke. NeuroReport, 2000, 11, 2957-2960.	1.2	121
224	Experience with carbon-11 choline positron emission tomography in prostate carcinoma. European Journal of Nuclear Medicine and Molecular Imaging, 2000, 27, 1415-1419.	2.1	206
225	Early Detection and Accurate Description of Extent of Metastatic Bone Disease in Breast Cancer With Fluoride Ion and Positron Emission Tomography. Journal of Clinical Oncology, 1999, 17, 2381-2381.	1.6	266
226	Preparation and evaluation of the rhenium-188-labelled anti-NCA antigen monoclonal antibody BW 250/183 for radioimmunotherapy of leukaemia. European Journal of Nuclear Medicine and Molecular Imaging, 1999, 26, 1265-1273.	6.4	48
227	Radiation doses of yttrium-90 citrate and yttrium-90 EDTMP as determined via analogous yttrium-86 complexes and positron emission tomography. European Journal of Nuclear Medicine and Molecular Imaging, 1996, 23, 958-966.	2.1	71